J MATER SCI 41 (2006) 2187–2193

Photocatalytic properties of the SBA-15 mesoporous silica molecular sieve modified with titanium

A. ORLOV, Q.-Z. ZHAI, J. KLINOWSKI*
Department of Chemistry, University of Cambridge, Lensfield Road, Cambridge CB2 1EW, U.K.
E-mail: jk18@cam.ac.uk

Published online: 6 April 2006

We describe three methods of post-synthesis modification of the SBA-15 mesoporous molecular sieve with titanium: impregnation with $Ti(OEt)_4$ in an ethanolic solution, grafting with titanocene dichloride, and modification with colloidal titania. The products were characterized using X-ray diffraction (XRD) and N_2 adsorption as well as Fourier-transform infrared and ^{29}Si NMR spectroscopies. All three methods yield materials containing 1.4–4.7 wt.% titanium and with high surface areas. The absorbance at 960 cm^{-1} in SBA-15 modified with colloidal titania and SBA-15 grafted with titanocene indicates the formation of Ti–O bonds. All products showed significant activity towards the degradation of p-chlorophenol. UV-vis absorption spectra of SBA-15 samples modified with titanium indicate that the variation in the photocatalytic activity is governed by isolated titanium sites.

1. Introduction

A range of titanium-containing microporous and mesoporous materials with high surface areas and high thermal stability has been prepared by post-synthesis methods in zeolites Ti-ZSM-5 [1] and Ti-FSM-16 [2] and during synthesis in Ti-MCM-41 [3–5] and Ti-MCM-48 [3, 6–9]. Post-synthetic procedures included grafting with metallocene complexes on mesoporous silica [10], impregnation [2] and ion exchange in Al-containing MCM-41 [11]. Chemical reactions catalysed by Ti-MCM-41 and Ti-HMS include epoxidation of alkenes, hydroxylation of phenol, oxidative aromatic bromination and carbohydrate oxidation [4, 12].

While the catalytic properties of Ti-MCM have been established, little is known about the photocatalytic activity of other mesoporous materials containing titanium. The photocatalitic activity of TiO_2 supported on hexagonal mesoporous silica is significantly increased in comparison with TiO_2 alone [13]. Ti-MCM-41 has an increased photocatalitic activity for oxidizing phenol in comparison with the activity of pure TiO_2 or composite Ti-Si oxides [14, 15]. Ti-MCM-41 and Ti-MCM-48 are also very active in the reduction of CO_2 with H_2O in the gas phase [3]. The catalytic activity is variously attributed to quantum size effects of extra-framework titania particles supported on silica [16], to increased adsorptivity towards an organic substrate [16] and to tetrahedrally coordinated Ti in the silica framework [3, 17].

SBA-15, a mesoporous molecular sieve with exceptionally wide (50–300 Å diameter) ordered channels [18–22], high surface area and high thermal stability, offers additional advantages as a catalyst and catalyst support. It can accommodate larger molecules than other molecular sieves and should allow a higher flow rate of reactants and products in and out of the pores. The grafting of Ti on SBA-15 [9, 23, 24] extends the range of application of this silica phase and prompts the study of alternative grafting and impregnation procedures. We describe three post-synthetic methods of preparation of SBA-15 modified with titanium, and the characterization of the products using XRD, N_2 adsorption, FTIR and ^{29}Si magic-angle-spinning (MAS) NMR spectroscopies. We also compare the photocatalytic properties of the products for the destruction of hazardous environmental pollutants, such as p-chlorophenol.

2. Experimental methods

2.1. Sample preparation

SBA-15 was synthesized as follows [21]. 2g of amphiphilic triblock copolymer, poly(ethyleneglycol)-block-poly(propyleneglycol)-block poly(ethyleneglycol) (average molecular weight 5800, Aldrich) was dispersed in 15 g of water and 60 g of 2M hydrochloric acid solution while stirring, followed by addition of 4.25 g of tetraethyl orthosilicate (Aldrich) to the homogeneous solution with stirring. The mixture was stirred at 40°C for

*Author to whom all correspondence should be addressed.
0022-2461
DOI: 10.1007/s10853-006-7184-5

24 h, and heated in a Teflon-lined autoclave at 100°C for 2 days. The solid product was then filtered, washed with deionized water, dried in air at room temperature and finally calcined in air at 550°C for 24 h to decompose the triblock copolymer to obtain SBA-15 as a white powder. Ti-modified SBA-15 was prepared by three different methods.

2.1.1. Method I

SBA-15 was impregnated with $Ti(OET)_4$ in an ethanolic solution (Aldrich) for 4 h and dried at room temperature [11].

2.1.2. Method II

A colloidal solution was prepared by hydrolysis of the tetraisopropoxide (Aldrich), $Ti(O\text{-}I\text{-}Pr)_4$. 25 ml of $Ti(O–I–Pr)_4$ was added to 4 ml of isopropanol, the mixture was added to 50 ml of distilled deionized water containing 2 ml of 70% HNO_3 under continuous stirring for 6 h at 75°C. The organic layer was removed and the remaining colloidal solution stored. The solution remained stable for several months.

The supported catalyst was prepared by mixing colloidal solutions of TiO_2 with the molecular sieve support. In a preparation of a supported photocatalyst, 0.3 g of support was saturated with 10 ml of water for 30 min, and mixed with 0.6 ml of TiO_2 solution for 1 h with stirring. The mixture was dried by evaporation at 50°C for 10 h, followed by heating at 120°C overnight and finally the solid was calcined at 450°C for 12 h. Several Ti-SBA-15 samples with different titanium content were prepared by this procedure [13].

2.1.3. Method III

Synthesis was performed under a nitrogen atmosphere in a Schlenk apparatus. 400 mg of SBA-15 were degassed at 120°C for 2 h. 200 mg of titanocene dichloride was dissolved in dry distilled chloroform and allowed to diffuse into SBA-15 for 30 min. SBA-15 was then exposed to triethylamine to activate the surface silanol groups. The suspension was stirred under a nitrogen atmosphere for 24 h, when the colour of SBA-15 gradually changed to yellow. After extensive washing with chloroform, the organic component was removed by calcination at 550°C for 24 h [10].

2.2. Sample characterization

N_2 adsorption isotherms were measured by the BET method using nitrogen as an adsorption gas at *77* K using a Coulter SA 3100 instrument. Samples were outgassed at 350°C for 12 h prior to surface area measurements. XRD was determined by small angle X-ray scattering (SAXS) with a computer controlled Kratky camera using Cu Kα ($\lambda = 1.5418$ Å) radiation at 40 kV and 40 mA. The size of the colloidal Ti particles was determined on desmeared XRD data on the basis of the Guinier plot.

The FTIR spectrum was recorded from KBr pellets (99 wt.% of KBr) on a Nicolet 205 FTIR spectrophotometer. Diffuse reflectance absorption was measured by a Shimadzu-3100 spectrophotometer.

^{29}Si MAS NMR spectra were measured at 79.5 MHz on a Chemagnetics CMX-400 spectrometer with zirconia rotor *7*.5 mm in diameter spun in air at 3.5 kHz. 60° radiofrequency pulses, 4 μs pulse width, and 410 s pulse delays were used. 100 scans were acquired. Chemical shifts were recorded relative to TMS. Elemental analysis was performed on a UNICAM 989 atomic absorption spectrometer.

2.3. Photocatalytic reactions

The photocatalytic reactions were conducted under identical conditions. 25 mg of the catalyst in 5 ml of deionized water were charged into a photochemical reactor. The mixture was sonicated for 10 min to give a highly dispersed catalyst. 20 ml of 50 mM aqueous solution of p-chlorophenol were then added to the reaction vessel. The mixture was irradiated for 3 h by a 120 W mercury lamp situated at the centre of the reactor, and encased in a quartz immersion well with a water jacket for temperature control. Pure oxygen was constantly bubbled through the reaction vessel. Losses due to sorption and volatilisation were accounted for by using a blank sample with unmodified SBA-15. After the end of the reaction the solution was centrifuged, diluted with methanol and analyzed by a Perkin Elmer Autosystem XL Turbomass GC/MS. The final chloride concentration was determined by titration with $AgNO_3$. The partial oxidation of p-chlorophenol without a catalyst in the presence of UV light was accounted for by subtracting chloride production and the disappearance of p-chlorophenol on unmodified SBA-15 from the catalytic results. Anatase (Aldrich) was used as a benchmark for the photocatalytic activity.

3. Results and discussion

3.1. XRD

The well-defined XRD pattern of parent SBA-15 was indexed on a hexagonal lattice (Table I) with unit cell parameter $a_o = 116$ Å($2\theta = 0.88°$). Only Ti-SBA-15 prepared with high loading of colloidal titania gave lower quality patterns than those of purely siliceous material, indicating a decrease of crystallinity. SAXS characterization of precursor colloidal solution indicated that the average size of colloidal particles is smaller than the pore diameter of SBA-15, suggesting that the nanoparticles could diffuse inside the mesoporous support. However, the possibility that some particles could agglomerate outside the support cannot be ruled out. All the other samples, i.e. SBA-15 impregnated with Ti in ethanolic solution, prepared with dilute colloidal titania and grafted with titanocene, gave XRD patterns similar to those of the parent SBA-15 (Fig. 1). This demonstrates successful incorporation of titanium into SBA-15 and the retention of its highly ordered hexagonal mesostructure, signifying the consider-

TABLE I Properties of SBA-15 and dilute colloidal titania modified Ti-SBA-15, alkoxide-impregnated Ti-SBA-15 grafted with titanocene. The unit cell parameter a_0 was calculated from XRD; pore size distribution and surface areas were determined from N_2 adsorption/desorption measurements. The content of Ti was determined by atomic absorption.

Sample	Unit cell parameter	BET surface area (m^2/g)	Pore volume (cm^3/g)	Pore volume (Å)	Titantium content (wt.%)
SBA-15	116	651	1.141	67.6	–
Ti-SBA-15	116	627	1.073	63.4	2.04
Ti-SBA-15 impregnated	116	609	1.042	63.4	1.42
Ti-SBA-15 grafted	116	525	0.94	63.4	4.73

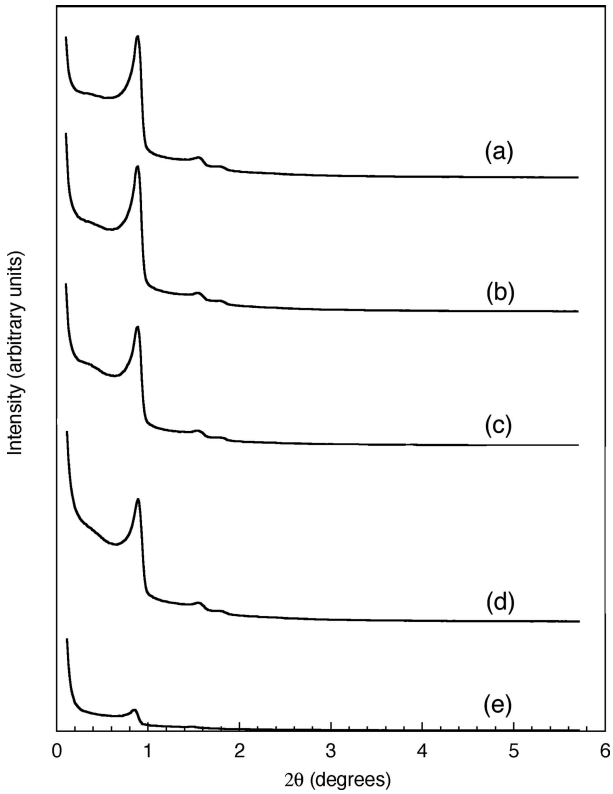

Figure 1 X-ray powder diffraction patters of (a) parent SBA-15; (b) alkoxide-impregnated Ti-SBA-15; (c) titanocene-grafted Ti-SBA-15; (d) dilute colloidal titania modified Ti-SBA-15; (e) concentrated colloidal titania modified Ti-SBA-15.

able stability of the materials. No higher-order reflections attributable to titania, such as peaks attributable to anatase at $2\theta = 25.3°(101)$ and to rutile at $2\theta = 27.3°(110)$, were observed, indicating the absence of bulk anatase or rutile.

3.2. Nitrogen adsorption

All materials gave type IV adsorption isotherms with H1-type hysteresis loop, according to IUPAC classification (Fig. 2). The surface area and effective pore diameters of parent SBA-15 and Ti-SBA-15 are summarised in Table I. The BJH pore size distribution curves calculated for SBA-15 and Ti-SBA-15 are shown in Fig. 3. SBA-15, and

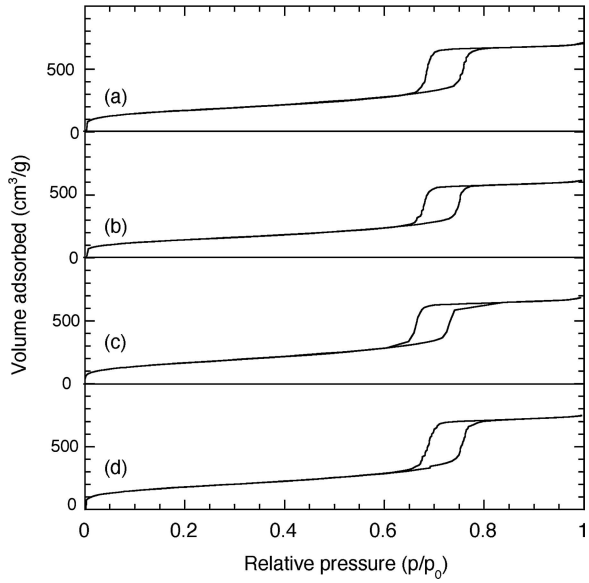

Figure 2 Adsorption/desorption isotherms of nitrogen for (a) dilute colloidal titania modified Ti-SBA-15; (b) titanocene-grafted Ti-SBA-15; (c) alkoxide-impregnated Ti-SBA-15; (d) parent SBA-15.

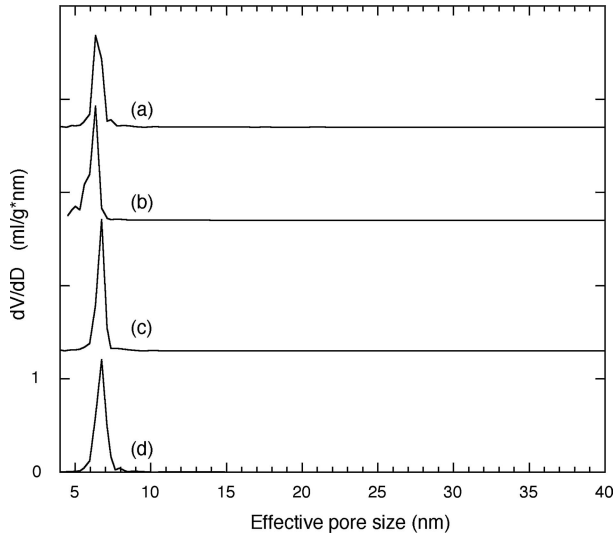

Figure 3 BJH pore size distribution calculated from the desorption branch of the isotherm for (a) titanocene-grafted Ti-SBA-15; (b) alkoxide-impregnated Ti-SBA-15; (c) dilute colloidal titania modified Ti-SBA-15; (d) parent SBA-15.

SBA-15 modified with titanium have a uniform pore size distribution, and a very small reduction in pore size and surface area. The largest reduction (ca. 20%) in surface area occurs for SBA-15 grafted with titanocene dichloride. This is consistent with the highest (ca. 4.7 wt.%) degree of titanium loading for this sample.

3.3. FTIR

Fig. 4 shows the FTIR spectra of purely siliceous and titanium-containing mesoporous materials. The asymmetric stretching vibrations (Si–O–Si) appear at 1085 cm^{-1} in the spectra of all the samples, and were not influenced by the presence of titanium. How-

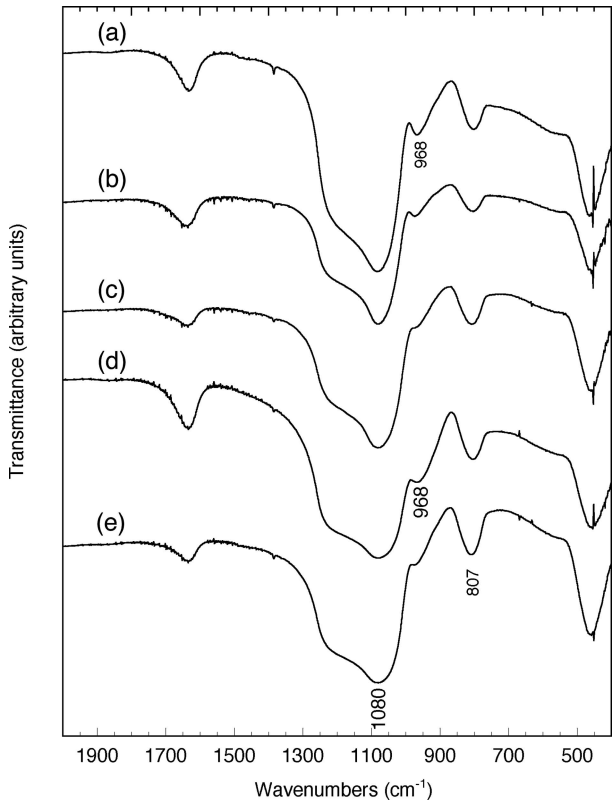

Figure 4 FTIR spectra of (a) concentrated colloidal titania modified Ti-SBA-15; (b) dilute colloidal titania modified Ti-SBA-15; (c) alkoxide-impregnated Ti-SBA-15; (d) titanocene-grafted Ti-SBA-15; (e) parent SBA-15.

ever, symmetric stretching vibrations at 807 cm^{-1} were shifted towards lower wavenumbers for all Ti-modified samples, except the SBA-15 impregnated with titanium. Appearance of the band at 968 cm−1 for titanium-modified SBA-15 [25] prepared with the low concentration of colloidal titanium is indicative of the formation of a Ti-O-Si bond. The intensity of the 968 cm^{-1} band increased with increased Ti content in the sample. Similarly, SBA-15 modified with titanocene also showed a peak at 968 cm^{-1}. On the other hand, FTIR spectra of SBA-15 impregnated with Ti from ethanolic solution was not significantly different from that of unmodified SBA-15. However, this does not necessarily imply the absence of Ti–O–Si bonds in SBA-15 impregnated with titanium. The fact that SBA-15 itself exhibits a shoulder at 968 cm^{-1} can be explained by the results reported by Blasco *et al.* [26], who suggested that in purely siliceous mesoporous materials this vibration is attributed to the abundance of silanol groups. The 968 cm^{-1} band cannot therefore be used as an absolute criterion of the presence of titanium in the framework for the lower Ti-content samples. The absence of a stretching band at 710 cm^{-1} in all samples indicates the absence of crystalline titanium dioxide.

3.4. UV-vis spectroscopy

Fig. 5 shows UV-vis absorption spectra of SBA-15 modified with titanium. No absorption due to framework silica

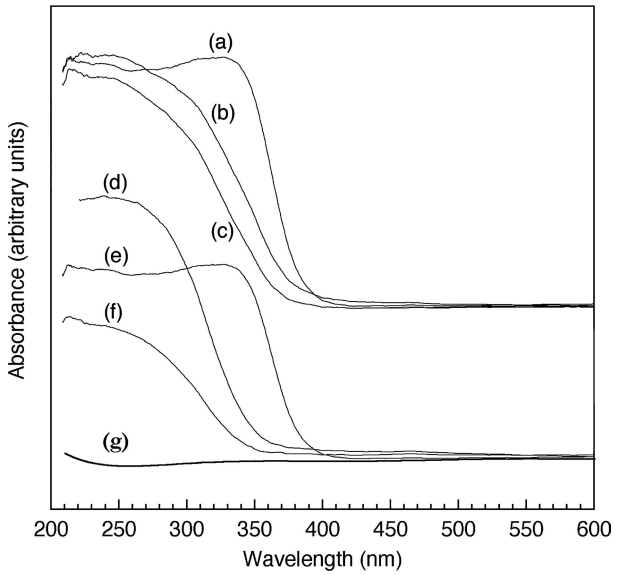

Figure 5 UV-vis spectra of (a) anatase; (b) concentrated colloidal titania modified Ti-SBA-15; (c) dilute colloidal titania modified Ti-SBA-15; (d) titanocene-grafted Ti-SBA-15; (e) anatase; (f) alkoxide-impregnated Ti-SBA-15; (g) parent SBA-15.

was observed. It is clear that the increase in titanium content for SBA-15 modified with colloidal titania caused a significant shift toward longer wavelengths. These samples had very broad absorption with two poorly resolved peaks at 212 and 244 nm, attributed to tetrahedrally and octahedrally coordinated isolated titanium species, respectively. These features are very similar to those found in TS-1 materials [27]. The increase in broad features of the spectra with the increase in titanium content can be

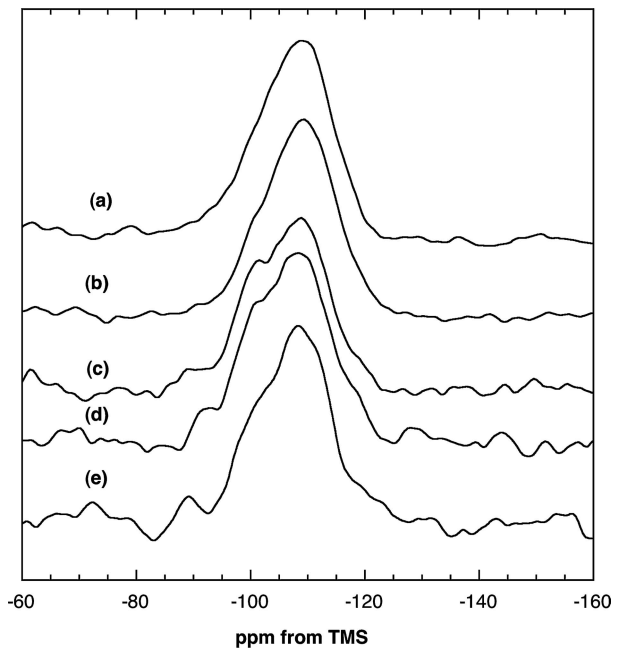

Figure 6 ^{29}Si MAS NMR spectra of (a) alkoxide-impregnated Ti-SBA-15; (b) titanocene-grafted Ti-SBA-15; (c) concentrated colloidal titania modified Ti-SBA-15; (d) dilute colloidal titania modified Ti-SBA-15; (e) parent SBA-15.

attributed to a decrease in isolated Ti(IV) framework sites and the appearance of oligomerized titanium species.

SBA-15 modified with titanocene dichloride gives a very broad peak with a maximum at 238 nm. SBA-15 impregnated with titanium had two poorly defined peaks at 212 and 241 nm. The intensity of the peak for SBA-15 modified with titanocene dichloride was much higher and the absorption band was much broader than for SBA-15 impregnated with titanium. A higher titanium content and higher degree of oligomerization for titanocene modified samples than those for samples impregnated with titanium is consistent with the observed features of UV-vis spectra. The results indicate that the concentration of isolated titanium sites is the highest in SBA-15 impregnated with titanium and the lowest for SBA-15 grafted with titanocene, with SBA-15 modified with dilute colloidal titania having a similar degree of oligomerization to SBA-15 grafted with titanocene. We note that no peaks at larger wavelengths (ca. 375 nm) were observed in any sample, indicating that microcrystalline TiO_2 with Ti in an octahedral environment and forming Ti–O–Ti bonds is absent.

3.5. Solid-state NMR

The "Q^n notation" is often adopted for the description of building units in silicates [28]. In this notation, Q stands for a silicon atom bonded to four oxygen atoms forming a SiO_4 tetrahedron. The superscript n indicates the connectivity, i.e. the number of other Q units attached to the unit in question and the central silicon atom is

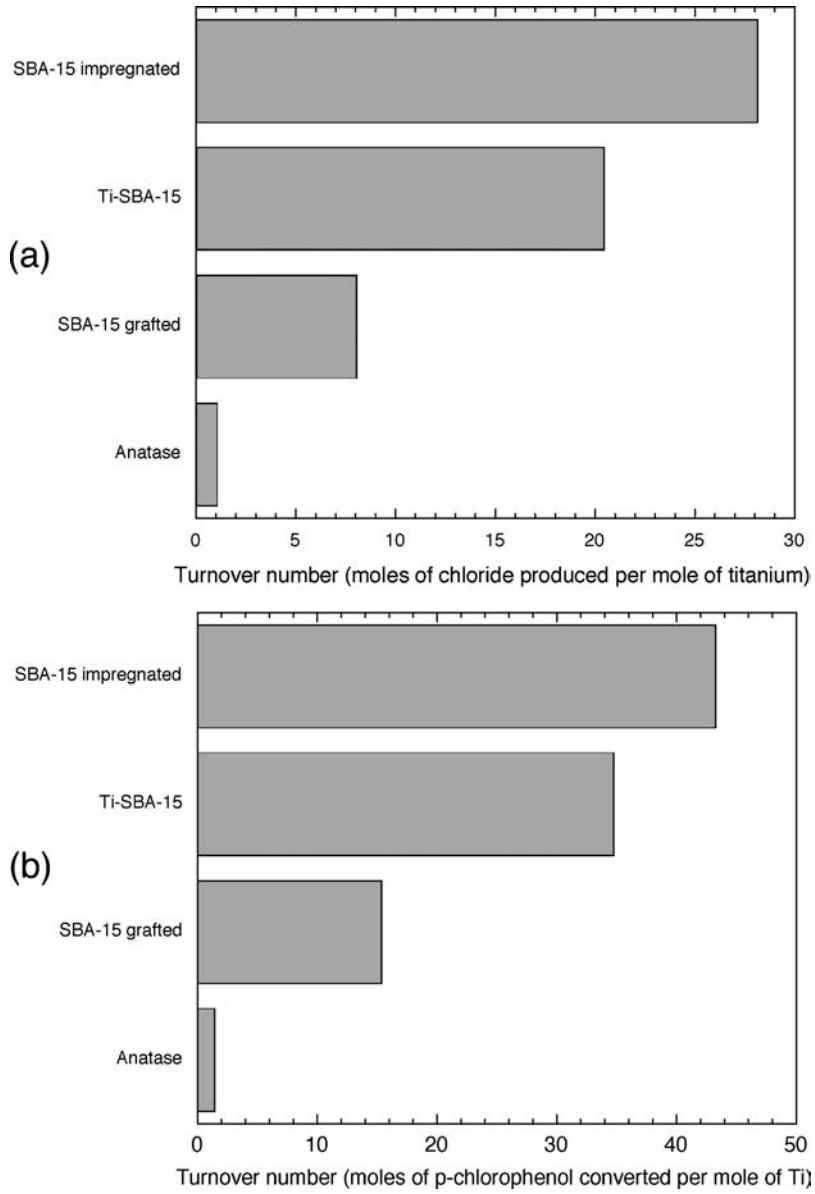

Figure 7 (a) Photocatalytic production of chloride ions on anatase; titanocene-grafted Ti-SBA-15; dilute colloidal titania modified Ti-SBA-15; alkoxide-impregnated Ti-SBA-15. (b) Photocatalytic conversion of p-chlorophenol on anatase; titanocene-grafted Ti-SBA-15; dilute colloidal titania modified Ti-SBA-15; alkoxide-impregnated Ti-SBA-15.

written in bold. The SiO_4 tetrahedron is 4 connected, and the remaining $(4 - n)$ units linked to it are often hydroxyl groups. Thus, Q^4 stands for three-dimensionally cross-linked **Si**$(OSi)_4$ units, Q^3 for **Si**$(OSi)_3(OH)$ units and Q^2 for **Si**$(OSi)_2(OH)_2$ units. ^{29}Si MAS NMR spectra (Fig. 6) show peaks at -92 ppm (Q^2), -100 ppm (Q^3) and -110 ppm (Q^4). The Q^3/Q^4 ratio is a measure of the extent of silanol condensation, and is zero for a fully condensed framework. The Q^3/Q^4 ratios are 0.22, 0.35, 0.39, 0.27 and 0.22 for parent SBA-15, SBA-15 modified with a low concentration of colloidal titanium, SBA-15 modified with concentrated colloidal titania, SBA-15 impregnated with $Ti(OET)_4$ and SBA-15 prepared by the addition of titanocene. The increased Q^3/Q^4 ratio in Ti-modified samples (except for SBA-15 prepared by the addition of titanocene and by impregnation from ethanolic solution) implies that the degree of condensation of silica walls in Ti-modified SBA-15 is slightly lower than that in parent SBA-15.

3.6. Photocatalytic testing

All three catalysts showed significant activity towards the degradation of p-chlorophenol. As the chloride ions are produced via partial or complete oxidation of p-chlorophenol, their concentration is a measure of the degree of degradation of the parent compound. Production of chloride ions was accompanied by the degradation of p-chlorophenol (Fig. 7). Higher turnover numbers for p-chlorophenol than for chloride production indicate that not all the p-chlorophenol is degraded, and that intermediate chlorinated products are formed.

It is likely that the higher activity of impregnated samples is attributable to high concentrations of isolated Ti(IV) framework, as illustrated by UV-vis absorption spectra. It also indicates that the enhanced presence of highly isolated titanium sites at low titanium loading might be necessary for high photocatalytic activity. These results are consistent with those of earlier demonstrations of the effect of tetrahedrally coordinated titanium on photocatalytic activity [14]. In addition, a sizeable reduction of the surface area of SBA-15 modified with titanocene may cause a further decrease in catalytic performance. However, the increased concentration of the chloride anions, coinciding with increased degradation of p-chlorophenol, indicates that the observed effects are not due to changes in adsorptive properties and that the coordination number of titanium is crucial to the trends observed.

4. Conclusions

1. Modification of SBA-15 with titanium by impregnation, grafting and treatment with colloidal titania resulted in the retention of highly ordered hexagonal mesostructures, signifying the great stability of SBA-15 even at high (4.7 wt.%) concentrations of titanium. The high degree of crystallinity was confirmed by XRD, with ^{29}Si MAS NMR showing only a small decrease in the degree of silica condensation. No difference in the asymmetric stretching vibration of Si–O–Si bonds due to titanium deposition was observed by FTIR. The surface area of the mesoporous materials remains unaffected by titanium deposition, except for samples containing 4.7 wt.% of titanium, where there was a 20% reduction in surface area.

2. Results from FTIR, and UV-vis spectroscopies suggests the formation of Ti–O–Si bonds, as well as the coexistence of 4- and 6-coordinated titanium in all samples. An increased titanium loading results in an increase in the content of 6-coordinated titanium and possibly in the oligomerization of titanium species. XRD, FTIR, and UV-vis indicate the absence of crystalline titanium dioxide from all samples.

3. All titanium-modified SBA-15 materials showed significant activity towards the catalytic degradation of p-chlorophenol. Increased degradation coincides with an increase in the production of chloride anions, indicating that the observed effects are not due only to changed adsorptive properties of SBA-15. The most active sample has enhanced concentration of isolated titanium sites, signifying that oligomerization of titanium is harmful to catalytic activity.

Acknowledgments

We are grateful to Dr. R. Mokaya, V. Golovko, Dr. Y. Khimyak, M. Vickers, S. Boreham and Dr. F. Benevelli for assistance. We thank the Cambridge University Overseas Trust for a grant to A.O.

References

1. B. SULIKOWSKI and J. KLINOWSKI, *Appl. Catal.* **A84** (1992) 141.
2. K. IKEUE, H. YAMASHITA and M. ANPO, *Chem. Lett.* (1999) 1135.
3. M. ANPO, H. YAMASHITA, K. IKEUE, Y. FUJII, S. G. ZHANG, Y. ICHIHASHI, D.R. PARK, Y. SUZUKI, K. KOYANO and T. TATSUMI, *Catal. Today* **44** (1998) 327.
4. P. T. TANEV, M. CHIBWE and T. J. PINNAVAIA, *Nature* **368** (1994) 321.
5. M. D. ALBA, Z. H. LUAN and J. KLINOWSKI, *J. Phys. Chem.* **100** (1996) 2178.
6. M. MOREY, A. DAVIDSON and G. STUCKY, *Microporous Mater.* **6** (1996) 99.
7. K. A. KOYANO and T. TATSUMI, *Chem. Commun.* (1996) 145.
8. J. V. WALKER, M. MOREY, H. CARLSSON, A. DAVIDSON, G. D. STUCKY and A. BUTLER, *J. Am. Chem. Soc.* **119** (1997) 6921.
9. M. S. MOREY, S. O'BRIEN, S. SCHWAR and G. D. STUCKY *Chem. Mat.* **12** (2000) 898.
10. T. MASCHMEYER, F. REY, G. SANKAR and J. M. THOMAS, *Nature* **378** (1995) 159.
11. A. HAGEN, D. WEI and G. HALLER, in: "Mesoporous Molecular Sieves" (Elsevier, Baltimore, 1998) p. 191.
12. H. VAN BEKKUM and K. R. KLOETSTRA, in: "Mesoporous Molecular Sieves" (Elsevier, Baltimore, 1998) p. 171.
13. Q. DAI, N. HE, K. WENG, B. LIN, Z. LU and C. YUAN, *J. Incl. Phenom. Macro.* **35** (1999) 11.

14. S. ZHENG, L. A. GAO, Q. H. ZHANG and J. K. GUO, *J. Mater. Chem.* **10** (2000) 723.
15. B. J. ARONSON, C. F. BLANFORD and A. STEIN, *Chem. Mat.* **9** (1997) 2842.
16. Y. M. XU, W. ZHENG and W. P. LIU, *J. Photochem. Photobiol. A* **122** (1999) 57.
17. H. YAMASHITA, S. KAWASAKI, Y. ICHIHASHI, M. HARADA, M. TAKEUCHI, M. ANPO, G. STEWART, M. A. FOX, C. LOUIS and M. CHE, *J. Phys. Chem.* **B102** (1998) 5870.
18. D. Y. ZHAO, J. L. FENG, Q. S. HUO, N. MELOSH, G. H. FREDRICKSON, B. F. CHMELKA and G. D. STUCKY, *Science* **279** (1998) 548.
19. D. Y. ZHAO, Q. S. HUO, J. L. FENG, B. F. CHMELKA and G. D. STUCKY, *J. Am. Chem. Soc.* **120** (1998) 6024.
20. D. Y. ZHAO, J. Y. SUN, Q. Z. LI and G. D. STUCKY, *Chem. Mat.* **12** (2000) 275.
21. Z. H. LUAN, M. HARTMANN, D. Y. ZHAO, W. Z. ZHOU and L. KEVAN, *ibid.* **11** (1999) 1621.
22. M. J. CHENG, Z. B. WANG, K. SAKURAI, F. KUMATA, T. SAITO, T. KOMATSU and T. YASHIMA, *Chem. Lett.* (1999) 131.
23. R. VAN GRIEKEN, J. AGUADO, M. J. LOPEZ-MUNOZ and J. MARUGAN, *J. Photochem. Photobiol. A* **148** (2002) 315.
24. M. J. LOPEZ-MUNOZ, R. VAN GRIEKEN, J. AGUADO and J. MARUGAN, *Catal. Today* **101** (2005) 307.
25. A. CORMA, *Chem. Rev.* **97** (1997) 2373.
26. T. BLASCO, A. CORMA, M. T. NAVARRO and J. P. PARIENTE, *J. Catal.* **156** (1995) 65.
27. A. CARATI, C. FLEGO, E. P. MASSARA, R. MILLINI, L. CARLUCCIO, W. O. PARKER and G. BELLUSSI, *Microporous Mesoporous Mat.* **30** (1999) 137.
28. G. ENGELHARDT and D. MICHEL, in: "High-resolution Solid-State NMR of Silicates and Zeolites" (John Wiley, Chichester, 1987).

Received 3 August
and accepted 29 September 2005